Inhibition of polyamine uptake potentiates the anti-proliferative effect of polyamine synthesis inhibition and preserves the contractile phenotype of vascular smooth muscle cells.

Grossi, Mario; Phanstiel, Otto; Rippe, Catarina; Swärd, Karl; Alajbegovic, Azra; Albinsson, Sebastian; Forte, Amalia; Persson, Lo; Hellstrand, Per; Nilsson, Bengt-Olof

Published in:
Journal of Cellular Physiology

DOI:
10.1002/jcp.25236

2015

Inhibition of polyamine uptake potentiates the anti-proliferative effect of polyamine synthesis inhibition and preserves the contractile phenotype of vascular smooth muscle cells

Mario Grossi[1], Otto Phanstiel [2], Catarina Rippe[1], Karl Swärd [1], Azra Alajbegovic[1], Sebastian Albinsson[1], Amalia Forte[3], Lo Persson[1], Per Hellstrand[1], Bengt-Olof Nilsson[1,*]

[1]Dept. of Experimental Medical Science, Lund University, Sweden; [2]Dept. of Medical Education, University of Central Florida, Orlando, Florida; [3]Dept. of Experimental Medicine, Second University of Naples, Italy

Running head: Inhibition of polyamine synthesis and uptake

Keywords: · cell proliferation, •contractile phenotype, •polyamine synthesis, •polyamine uptake, •restenosis, •vascular smooth muscle cells

Total number of figures: 9
Total number of tables: 0

Conflict of interest: The authors declare no conflict of interest.

Contract grant sponsor: Swedish Research Council
Contract grant sponsor: Swedish Dental Society
Contract grant sponsor: Thuréus Foundation
Contract grant sponsor: Greta and Johan Kock Foundation

***Correspondence to**: Dr. Bengt-Olof Nilsson
Department of Experimental Medical Science
Lund University,
BMC D12
SE–221 84 Lund
Sweden
Phone: +46-46-2227767
Fax: +46-46-2224546
E-mail: bengt-olof.nilsson@med.lu.se

Abstract

Increased vascular smooth muscle cell (VSMC) proliferation is a factor in atherosclerosis and injury-induced arterial (re)stenosis. Inhibition of polyamine synthesis by α-difluoro-methylornithine (DFMO), an irreversible inhibitor of ornithine decarboxylase, attenuates VSMC proliferation with high sensitivity and specificity. However, cells can escape polyamine synthesis blockade by importing polyamines from the environment. To address this issue, polyamine transport inhibitors (PTIs) have been developed. We investigated the effects of the novel trimer44NMe (PTI-1) alone and in combination with DFMO on VSMC polyamine uptake, proliferation and phenotype regulation. PTI-1 efficiently inhibited polyamine uptake in primary mouse aortic and human coronary VSMCs in the absence as well as in the presence of DFMO. Interestingly, culture with DFMO for 2 days substantially (>95%) reduced putrescine (Put) and spermidine (Spd) contents without any effect on proliferation. Culture with PTI-1 alone had no effect on either polyamine levels or proliferation rate, but the combination of both treatments reduced Put and Spd levels below the detection limit and inhibited proliferation. Treatment with DFMO for a longer time period (4 days) reduced Put and Spd below their detection limits and reduced proliferation, showing that only a small pool of polyamines is needed to sustain VSMC proliferation. Inhibited proliferation by polyamine depletion was associated with maintained expression of contractile smooth marker genes. In cultured intact mouse aorta, PTI-1 potentiated the DFMO-induced inhibition of cell proliferation. The combination of endogenous polyamine synthesis inhibition with uptake blockade is thus a viable approach for targeting unwanted vascular cell proliferation *in vivo*, including vascular restenosis.

Introduction

The polyamines putrescine (Put), spermidine (Spd) and spermine (Spm) are necessary for cell proliferation (Pegg, 1988). Put is formed from the amino acid ornithine in a reaction catalyzed by ornithine decarboxylase (ODC). Spd and Spm are formed from Put via addition of first one and then a second aminopropyl group using spermidine synthase and spermine synthase, respectively. The chemical structure of Put, Spd and Spm is shown in figure 1. The intracellular polyamine levels are tightly regulated by *de novo* synthesis, degradation, and uptake of circulating polyamines. Many cancer cell types need high levels of polyamines to sustain their excessive proliferation rate, and accordingly show high activity of ODC and also high polyamine uptake (O´Brien, 1976; DiGiovanni, 1992; Weis et al., 2002; Linsalata et al., 2002). The ODC inhibitor DFMO has been intensively evaluated in human clinical trials as an anti-cancer and chemopreventive agent (Meyskens and Gerner, 1999; Levin et al., 2000; Levin et al., 2003; Meyskens et al., 2008). However, cancer cells may overcome polyamine depletion in response to DFMO treatment by importing polyamines obtained from diet or the intestinal microbial flora and delivered through the bloodstream (Sarhan et al., 1989). Thus, for sustained therapeutic depletion of cellular polyamines it is important to target not only endogenous synthesis of polyamines but also their cellular uptake.

Vascular smooth muscle cells (VSMCs) residing in the vascular wall are normally in a quiescent "contractile" phenotype with a low rate of proliferation. They can, however, transform to a "synthetic" phenotype with a high rate of proliferation and diminished expression of contractile and cytoskeletal proteins (Owens, 1995). This typically occurs in atherosclerosis and in response to vascular injury such as restenosis after arterial revascularization (Owens et al., 2004). Hence, similar to cancer development this vascular pathology implies an increase in proliferative capacity, but in contrast to cancer the phenotype switching of VSMCs is generally reversible. In the clinical management of restenosis, stents and balloons coated with anti-cancer drugs such as the microtubule disruptor paclitaxel are widely used (Wessely, 2010). Due to unwanted side-effects and therapeutic resistance, there is a strong need for new and effective anti-proliferative drugs with low toxicity to combat restenosis. Like other cells, VSMCs need polyamines to sustain their rate of proliferation (Odenlund et al., 2009; Grossi et al., 2014a). Lowering VSMC polyamine levels with DFMO may represent an alternative method to address the unwanted VSMC proliferation observed in restenosis (Forte et al., 2013). Such a strategy, however, would also need to target polyamine import processes because upregulated polyamine uptake in the presence of DFMO can compensate for inhibited polyamine synthesis (Grossi et al., 2014b). Therefore, developing a combination therapy involving DFMO and a polyamine transport inhibitor (PTI) was warranted.

The import of polyamines has been demonstrated and characterized in bacteria and single cellular eukaryotes (Miller-Fleming et al., 2015), but polyamine uptake in mammalian cells is less well understood. In fact, in mammalian cells no single polyamine transporter has yet been identified. There are two current models for polyamine transport, one involving a plasma membrane transporter (Soulet et al., 2002; Soulet et al., 2004; Poulin et al., 2012) and the other using a caveolin-dependent endosomal trafficking pathway (Belting et al., 1999; Belting et al., 2003; Welch et al., 2008). Different transporters belonging to the family of solute carrier transporters, such as the SLCs and CCC9, and the organic cation transporter 6 (OCT6) have been implicated in polyamine uptake mechanisms (Igarashi et al., 2010; Poulin et al., 2012; Abdulhussein et al., 2014). Uemura et al. (2010) demonstrated that the solute carrier transporter Slc3a2 mediates polyamine uptake in intestinal epithelial cells through a caveolin-1 (Cav-1)-dependent mechanism. It has also been reported that polyamine uptake is mediated by Cav-1-dependent endocytosis in colon cancer cells (Roy et al., 2008). Another candidate involves Slc7a1/CAT-1 belonging to the cationic amino acid transporter (CAT) family, which is widely expressed in mammalian tissues (Palacin et al., 1998; Yang et al., 2007). This CAT system can transport basic amino acids including lysine, arginine and

ornithine but might also accept polyamines as substrates because of the similarity in structure as well as in transport characteristics between basic amino acids and polyamines (Sharpe and Seidel, 2005). However, overexpression of CAT-1 in polyamine-transport deficient cells affected amino acid but not polyamine uptake, and consequently it was concluded that a common transporter involves an as yet unknown member of the CAT family (Sharpe and Seidel, 2005).

Polyamine transport inhibitors (PTIs) have been synthesized to counteract the induced polyamine uptake under DFMO-treatment. In this study, we investigate a novel and potent polyamine transport inhibitor N1,N1′,N1″-(benzene-1,3,5-triyltris(methylene))tris(N4-(4-(methylamino)butyl)butane-1,4-diamine (PTI-1) (Muth et al., 2014). The chemical structure of PTI-1 is shown in figure 1. We hypothesize that the combination therapy with DFMO+PTI would be very effective in depleting intracellular polyamine levels and limiting VSMC proliferation. The results show that PTI-1 efficiently inhibits polyamine uptake, but does not affect basic polyamine levels or cell viability when give alone. Furthermore, a very small pool of polyamines persisting during DFMO treatment is sufficient to support cell proliferation, but the combination with PTI-1 inhibits proliferation while reducing Put and Spd contents below the detection limit. These results encourage the combination of endogenous polyamine synthesis inhibition with polyamine uptake blockade in proliferative pathological settings *in vivo*, including vascular restenosis.

Materials and Methods

Animals

C57BL/6 mice were purchased from Scanbur (Karlslunde, Denmark) and matched for sex and age. Cav-1 KO mice were obtained from the Jackson Laboratory (Bar Harbor, ME, USA), backcrossed on C57BL/6 (Grossi et al., 2014b) and maintained in homozygous breeding at the local animal facility at BMC, Lund, Sweden. Mice had free access to standard chow and water and were euthanized with CO_2. All experiments were approved by the local Animal Ethics committee in Lund/Malmö (M433-12).

Cells and cell culture

Aortas were isolated and incubated for 30 min at 37^{o}C in serum-free DMEM cell culture medium containing 1 mg/mL collagenase type 2 (Worthington Biochemical Corporation). The adventitia was then pulled off using forceps and the aortas were incubated for another 2 h in DMEM with 2 mg/mL collagenase type 2 and 0.2 mg/mL elastase (Sigma). Primary human coronary smooth muscle cells were purchased from Gibco. The VSMCs were cultured in DMEM medium with addition of antibiotics (50 U/mL penicillin and 50 µg/mL streptomycin) and 10% fetal bovine serum (FBS), and were trypsinized (0.25% trypsin) upon reaching confluence. The cells were used in passages 2-6. They grew in a "hill and valley pattern" (Chamley-Campbell et al., 1979) typical for VSMCs and were characterized by positive staining for the smooth muscle cell markers calponin and SM22α. The VSMCs were kept in a water-jacketed cell incubator at 5% CO_2 in air at 37°C.

Measurement of polyamine, arginine uptake and polyamine contents

The cells were pulse-labeled with radioactive ([^{3}H]) Put (10 µM), Spd (5 µM) or arginine (1 μCi) for 30 min at 37℃. The incubation was terminated by placing the cell dishes on ice followed by washing twice with PBS. The cells were lysed in 0.5 M NaOH and radioactivity was measured in a liquid scintillation counter (Beckman). Radioactivity was expressed as disintegrations per minute and normalized to the total protein concentration in each sample. Protein concentration was determined using a Bio-Rad protein assay kit based on the Lowry method (Lowry et al., 1951). For polyamine analysis, cells were washed in PBS, harvested using 0.25% trypsin, and then centrifuged at 2880 g for 5 min at room temperature. The cell pellets were sonicated twice for 10 s in PBS, and aliquots were mixed with equal volumes of 0.4 M perchloric acid, incubated at 4℃ for 30 min and then centrifuged at 18000 g for 2 min at room temperature. Chromatographic separation and quantitative determination of the polyamines in the cell extracts were done with high-performance liquid chromatography (HPLC, Hewlett Packard 1100) with o-phthalaldehyde as the reagent (Grossi et al., 2014b). Cellular polyamine contents were normalized to total protein concentration in each sample.

Assessment of cell proliferation and density

Cell proliferation was evaluated by measuring cell viability using the Cell Counting Kit-8 (CCK-8, Dojindo, Kumamoto, Japan) assay according to the manufacturer's instructions. Briefly, cells were

incubated with 10 µL CCK-8 reagent for 2.5 h at 37° C in a 96-well plate, and then absorbance at 450 nm was measured on an automated plate reader (Multiskan GO, Thermo Scientific). Each sample was analyzed in triplicate.

Cell density was determined by nuclear staining with crystal violet. The cells were fixed in Hank´s balanced salt solution containing 1% glutaraldehyde for 30 min and then incubated with 0.1% crystal violet for 30 min at room temperature. Unbound dye was removed by gently rinsing the plates in deionized water. The plates were air dried and inspected under a microscope. To dissolve the crystal violet pigments, 10% acetic acid was included for 5 min under gentle shaking. The absorbance at 595 nm was recorded using the microplate reader.

Quantitative real-time RT-PCR

Total RNA was isolated using miRNeasy mini kit (Qiagen), including on-column DNAse I digestion according to the manufacturer's instructions. The relative expression of target genes was analysed by one step quantitative real-time RT-PCR (StepOnePlus qPCR cycler, Applied Biosystems) using QuantiFast SYBR Green RT-PCR Kit (Qiagen, 204156) applying Gapdh as housekeeping gene (Pfaffl, 2001). The following QuantiTect primer assays (Qiagen) were used: Gapdh (Mm_Gapdh_3_SG, QT01658692), Slc3a2 (Mm_Slc3a2_1_SG, QT00109914), Slc7a1 (Mm_Slc7a_1__1_SG, QT00099799), Cnn1 (Mm_Cnn1_1_SG, QT00105420), Tagln (Mm_Tagln_1_SG, QT00165179) and Spp1 (Mm_Spp1_1_SG, QT00157724).

Immunochemistry and EdU proliferation assay

Vessels were fixed in 4% buffered formaldehyde, dehydrated and embedded in paraffin. Five micrometer cross-sections were dewaxed, rehydrated with descending concentrations of ethanol and rinsed in distilled water. The antigen for von Willebrand factor (vWF) and calponin/SM22α was retrieved, respectively, with proteinase K and trypsin treatments. Tissue sections were stained with the polyclonal rabbit SM22α (Abcam, 1:200), calponin (Abcam, 1:200) and vWF (Dako, 1:500) antibodies. The immunoreactive signal was visualized using secondary antibodies conjugated Alexa-Fluor-488 (Life Technologies) or Alexa-Fluor-555 (Invitrogen) at 1:200 dilution.

EdU staining was conducted using Click-iT™ EdU imaging kit (Invitrogen) according to the manufacturer's protocol. Cross sections were permeabilized with 0.5% Triton X-100 for 20 min, the sections were washed twice with 3% bovine serum albumin (BSA) in PBS and then incubated with a Click-iT™ reaction cocktail containing Click-iT™ reaction buffer, $CuSO_4$, Alexa Fluor® 488 Azide, and reaction buffer additive for 30 min while protected from light. The sections were washed once more with 3% BSA and left in 3% BSA for 30 min more.

The nuclei were counterstained with DAPI (Invitrogen). Fluorescence signal was analysed using an Olympus DP72 microscope equipped with a digital camera. The Olympus CellSensDimension software was used for morphometric analysis.

Drugs

DFMO was kindly provided by Hoechst Marion Roussel, Cincinnati, OH, USA. PTI-1 was synthesized and provided by Otto Phanstiel´s laboratory at UCF in Orlando, Florida. Both DFMO and PTI-1 were dissolved in PBS.

Statistical analysis

Summarized data are presented as means ± SEM. For experiments using cultured cells, each culture dish represents one biological replicate, i.e. one observation (n=1). Statistical significance was calculated by Student´s t-test for single comparisons and by one-way ANOVA followed by Bonferroni's multiple comparison test for post hoc analysis as appropriate (GraphPad Software, Inc., San Diego, CA, USA). P-values < 0.05 were considered significant.

Results

The PTI-1 compound inhibits polyamine uptake in mouse VSMCs

The impact of PTI-1 on polyamine uptake was investigated in mouse VSMCs incubated with or without 5 mM DFMO for 2 days and then pulse labelled with [^{3}H]Put or [^{3}H]Spd in the presence or absence of increasing concentrations of PTI-1. Treatment with DFMO (1-10 mM) has previously been shown to inhibit VSMC polyamine formation without any impact on cell viability (Odenlund et al., 2009). DFMO-treatment increased basal Put and Spd import by about two-fold, whereas PTI-1 inhibited uptake of both polyamines in a concentration-dependent manner (Fig. 2A and B). The DFMO-enhanced Put uptake was completely prevented by PTI-1 at concentrations >1 μM, while DFMO-enhanced Spd uptake was slightly less sensitive. PTI-1 (0.025-3 μM) had no effect on DNA synthesis, assessed by measurement of [^{3}H]-thymidine incorporation, demonstrating that PTI-1 alone at these concentration has no toxic effect (data not shown). In the following experiments, 0.5 μM PTI-1 was used, a concentration that almost completely blocks both basal and DFMO-induced Put and Spd uptake. PTI-1 inhibited both basal and DFMO-induced Put and Spd uptake also in VSMCs cultured under growth-arrested (0.1 % FBS) conditions (data not shown).

Degradation of polyamines by serum oxidases may affect the amount of radio-labelled Put and Spd available for uptake. Therefore, we performed control experiments measuring Put and Spd uptake in the presence of the diamine oxidase inhibitor aminoguanidine. Uptake of [^{3}H]-Put and [^{3}H]-Spd was similar both in the presence and absence of 0.25 mM aminoguanidine (data not shown). Uptake of polyamines and the polyamine precursor arginine have been suggested to share a common mechanism (Abdulhussein et al., 2014), and, therefore, we measured uptake of [^{3}H]-labelled arginine. DFMO decreased arginine uptake by about 20% compared with control cells, possibly reflecting decreased cellular arginine utilization (data not shown). Treatment with PTI-1 alone or in combination with DFMO had no effect on arginine-uptake (data not shown).

Cav-1 negatively regulates polyamine uptake in VSMCs, resulting in increased basal as well as DFMO-stimulated polyamine uptake in Cav-1 KO relative to wild-type mice (Grossi et al., 2014b), PTI-1 reduced basal and completely prevented DFMO-induced polyamine uptake in Cav-1 knockout VSMCs (Fig. 3). Both the caveolin-1- and DFMO-regulated polyamine uptake components are thus sensitive to PTI-1.

Severely reduced cellular Put and Spd levels are needed to inhibit vascular smooth muscle cell proliferation

Next, we studied the impact of DFMO and PTI-1, alone and in combination, on mouse VSMC proliferation and polyamine contents. Treatment with either DFMO (5 mM) or PTI-1 (0.5 μM) for 2 days did not affect cell proliferation determined by CCK-8 assay and crystal violet staining, but the combined treatment with DFMO and PTI-1 reduced cell proliferation by about 35% (Fig. 4 A and B). Treatment with 5 mM DFMO for 2 days reduced Put and Spd levels by at least 95%, while treatment with PTI-1 alone had no effect on polyamine levels (Fig. 4 C and D). Importantly, the combination of DFMO with PTI-1, reduced both Put and Spd levels below the detection limit (Fig. 4 C and D). Since cells have significant stores of polyamines, depletion of intracellular polyamine levels by DFMO is expected to be a slow process. To address this issue, we examined cell proliferation and polyamine contents following a prolonged time exposure to DFMO. Treatment with DFMO (5 mM) for 4 days reduced mouse VSMC proliferation by about 50% (Fig. 5 A and B). Combination of DFMO with PTI-1 (0.5 μM) reduced proliferation more than treatment with DFMO alone (Fig. 5 A and B). The reduction of proliferation by DFMO alone or in combination with PTI-1 was associated with severe reduction of intracellular Put and Spd levels below the detection limit

(Figure 5 C and D). Treatment with DFMO and PTI-1 alone or in combination for either 2 or 4 days had no effect on VSMC Spm levels (data not shown).

Taken together these data indicate that only a very small pool of Put and/or Spd is needed to sustain VSMC proliferation.

Effects of treatment with DFMO and PTI-1 on VSMC gene expression

To evaluate the biological impact of inhibiting both endogenous synthesis and uptake of polyamines, we checked the mRNA levels of selected genes after 2 days of treatment with DFMO (5 mM) and PTI-1 (0.5 μM) (Fig. 6). The membrane transporters Slc3a2 and Slc7a1 (also known as CAT-1), belonging to the family of solute carriers, are potentially involved in polyamine uptake (Poulin et al., 2012). Both Slc3a2 and, especially, Slc7a1 gene expression was up-regulated similarly by DFMO and DFMO+PTI-1 treatment (Fig. 6). DFMO potentiated the expression of the smooth muscle contractile markers *Cnn1* (calponin) and *Tagln* (SM22α) (Fig.6). The combination of DFMO with PTI-1 gave no additional effect. *Spp1*, coding for osteopontin, is suggested to be involved in the shift of VSMCs from a contractile to a synthetic phenotype (Wolak et al., 2014). The *Spp1* gene was down-regulated by DFMO alone and in combination with PTI-1 (Fig. 6), providing additional evidences that inhibition of polyamine synthesis and uptake promotes the contractile phenotype in parallel with inhibition of proliferation.

Treatment with DFMO and PTI-1 in combination inhibits proliferation in human VSMCs

Next, we investigated the impact of PTI-1 in human VSMCs to see if PTI-1 represents a general concept for inhibiting polyamine uptake and proliferation. Treatment of primary human coronary smooth muscle cells with 5 mM DFMO for 2 days caused a 5- and 2.5-fold induction of Put and Spd import, respectively (Fig. 7 A and B). PTI-1 (0.5 μM) completely inhibited the DFMO-induced Put and Spd uptake (Fig. 7A and B). Treatment with PTI-1 reduced basal polyamine uptake as well. Treatment with either DFMO (5mM) or PTI-1 (0.5 μM) for 2 days did not affect human VSMC proliferation as determined by CCK-8 assay and crystal violet staining (Fig. 7 C and D). However, the combined treatment with DFMO and PTI-1 reduced human VSMC proliferation by about 35%, similar to the findings in mouse VSMCs.

DFMO and PTI-1 act in synergy to inhibit VSMC proliferation in cultured mouse aorta

Aorta organ culture has been widely used as an *ex vivo* model for studying vessel pathophysiology including endothelial dysfunction, vasoconstriction, and proliferation of VSMCs in their tissue and matrix environment. The organ culture experiments reported here were done in the presence of insulin (10 nM) and a low concentration (2%) of dialyzed FBS, a combination we have previously found to be suitable for preserving contractility (Zeidan et al., 2003). To evaluate the potential effect of the combination of DFMO and PTI-1 on VSMC proliferation, we cultured mouse aortic rings for 3 days in the presence or absence of DFMO (5 mM) or PTI-1 (1 μM) alone or in combination. The expression of smooth muscle (calponin/SM22α) and endothelium (vWF) differentiation marker expression at the protein level were not affected by treatment with DFMO and PTI-1 alone or in combination within this time frame (Fig. 8).

Consecutive sections to the ones used for immunohistochemistry were used to check the proliferation rate in the vascular media layer by EdU-assay. Treatment with DFMO alone and the combination of DFMO and PTI-1 were both effective in reducing VSMC proliferation in intact tissue, with a significantly larger effect of the combination (Fig. 9 A and B). Even though effects of

polyamine manipulation on proliferation rate were detected, the incubation time of 3 days was insufficient to produce measurable morphological effects, as evidenced by unaltered number of VSMC nuclei (Fig. 9 C). No effects of PTI-1 and DFMO treatment on lumen area, media area or media thickness were observed following this short culture period (data not shown).

Discussion

In this study we explored the importance of polyamine uptake for VSMC proliferation using a novel polyamine transport inhibitor (PTI-1). We demonstrate that the combined treatment with PTI-1 and the polyamine synthesis inhibitor DFMO effectively and specifically antagonizes VSMC proliferation both *in vitro* and *ex vivo*. Importantly, DFMO + PTI-1 inhibits proliferation and polyamine uptake in human as well as mouse VSMCs. The PTI-1 compound has been thoroughly characterized in human pancreatic cancer cells, showing high potency (EC_{50}=1.4 μM) for inhibiting the uptake of spermidine, low sensitivity to amine oxidases and low toxicity (Muth et al., 2014). An alternative approach for reducing intracellular polyamines is to find synthetic analogues of polyamines that compete with the import of natural polyamines but do not replace their function and, moreover, have the capacity to decrease natural polyamine levels by increasing their catabolism (Nowotarski et al., 2013). However, increasing polyamine catabolism may lead to increased formation of toxic metabolites including aldehydes and H_2O_2 (Wood et al., 2007; Pegg, 2013), representing a major disadvantage of this approach. Another limitation to the use of polyamine analogues is that they may inhibit their own import via induction of antizyme, which reduces uptake of the polyamine analogues (Mitchell et al., 2004). Thus, DFMO+PTI-1 combination may circumvent these issues especially if PTI-1 acts as a competitive inhibitor outside of cells. Future studies will be needed to better understand the role of antizyme during treatment of DFMO in combination with PTI-1.

Local application of DFMO inhibits smooth muscle proliferation without affecting the endothelial layer in rats exposed to a carotid lesion (Forte et al., 2013). This prior study, provided proof of principle for polyamines as a therapeutic target in this setting. Studies in cultured rat tail artery rings showed that DFMO counteracts the proliferation and loss of contractile differentiation caused by culture with FBS as a growth stimulant (Grossi et al., 2014a). The present data show that the combination of DFMO with PTI-1 more rapidly and potently attenuates VSMC proliferation than treatment with DFMO alone. Drug-eluting stents and balloons remain active for only a limited time after insertion, and thus it is important to keep the time of onset as short as possible (Wessely, 2010). Stents and balloons releasing the combination of DFMO and PTI-1 may represent a therapeutic option providing rapid and effective VSMC anti-proliferation.

The structure of the vascular wall is well maintained during polyamine depletion as demonstrated by unaltered endothelial expression of vWF and by expression of contractile phenotype marker proteins such as calponin and SM22α in the vessel media *ex vivo* and *in vivo* (present results, and Forte et al., 2013). At the mRNA level *Cnn1* and *Tagln*, coding for these proteins, were increased whereas *Spp1*, coding for the synthetic phenotype marker osteopontin (Wolak, 2014), was decreased by DFMO as well as by its combination with PTI-1. This likely represents a reversal towards a more contractile phenotype of the cultured VSMCs under growth stimulation by 10% FBS. At 2 days of culture, cell proliferation was inhibited only when DFMO was combined with PTI-1, whereas at 4 days DFMO alone reduced proliferation, potentiated by the addition of PTI-1. This suggests that the small pool of polyamine remaining at 2 days of treatment with DFMO is sufficient to support proliferation. Both treatments, however, had a similar effect on smooth muscle marker expression at 2 days, supporting the notion that DFMO started to depress signals for proliferation by this time point. Competition by proliferative mediators for the expression of smooth muscle genes has been demonstrated (Wang et al., 2004).

In several clinical trials, DFMO has been administered to cancer patients as a chemotherapeutic agent. It has the advantage of low toxicity and oral bioavailability which makes the drug particularly suitable for therapeutic use (Pegg, 1988; Meyskens and Gerner, 1999). The disadvantage of DFMO is that the drug activates the uptake of polyamines which allows the cancers

to circumvent its inhibition of polyamine biosynthesis. This is consistent with our observations in cultured VSMCs. The import-facilitated escape pathway may explain why the mouse and human VSMCs are resistant to acute treatment with DFMO alone for 2 days, and that a rather long-term (4 days) administration is required to deplete cellular polyamines sufficiently for inhibiting VSMC proliferation. Interestingly, treatment with DFMO for 2 days reduces VSMC polyamine contents by more than 95% but leaves a small residual fraction able to support cell proliferation. Inclusion of PTI-1 depletes VSMC polyamine contents below the detection limit of our assay, suggesting that this DFMO-resistant polyamine pool is dependent on cellular uptake. For the VSMCs in culture, the polyamines present in culture medium and available for uptake are probably released from the cells rather than introduced through supplementation of the culture medium with 10% FBS, since no polyamines are detected by HPLC analysis in the batches of FBS used for the present experiments (data not shown).

Treatment with DFMO not only enhances gene expression of the contractile markers calponin and SM22α but also increases expression of the putative polyamine transporters Slc3a2 and Slc7a1 (CAT-1). Interestingly, both Slc3a2 and Slc7a1 show a rapid increase in mRNA levels after vascular injury (Forte et al., 2008). Administration of PTI-1 alone (at 0.5 μM) has no effect on the expression of these genes, and, furthermore, PTI-1 had no effect on the DFMO-evoked up-regulation of Slc3a2 and Slc7a1. The DFMO-induced up-regulation of these Slcs is probably due to lowered cellular Put and Spd levels. Treatment with DFMO *in vivo* has been reported to have no effect on cellular levels of ornithine in various tissues making it less likely that ornithine regulates Slc3a2 and Slc7a1 expression (Seiler et al., 1989). On the whole, our data show that PTI-1 (at 0.5 μM) inhibits polyamine uptake but has no effects on gene expression either for genes coding for smooth muscle contractile marker proteins or genes coding for putative polyamine transporters. Importantly, these data suggest that PTI-1 specifically blocks polyamine uptake at the plasma membrane level, presumably as a competitive inhibitor at the cell surface, and has no intracellular effects. The inhibitor thus works synergistically with DFMO by a completely separate mechanism to reduce intracellular polyamine levels.

In conclusion, our data demonstrate that treatment with the combination of DFMO and PTI-1 depletes VSMC polyamine contents more efficiently than DFMO alone, inhibits VSMC cell proliferation, and maintains the VSMCs in a contractile phenotype. These results suggest that the combination of polyamine biosynthesis inhibitors and polyamine uptake inhibitors may be of significant therapeutic value in proliferative pathological settings *in vivo*, including vascular restenosis.

Acknowledgements

We thank Ina Nordström for excellent technical assistance.

References

Abdulhussein AA, Wallace HM. 2014. Polyamines and membrane transporters. Amino Acids 46:655-660.

Belting M, Persson S, Fransson LA. 1999. Proteoglycan involvement in polyamine uptake. Biochem J 338:317-323.

Belting M1, Mani K, Jönsson M, Cheng F, Sandgren S, Jonsson S, Ding K, Delcros JG, Fransson LA. 2003. Glypican-1 is a vehicle for polyamine uptake in mammalian cells: a pivital role for nitrosothiol-derived nitric oxide. J Biol Chem 278: 47181-47189.

Chamley-Campbell JH, Campbell GR, Ross R. 1979. The smooth muscle cell in culture. Physiol Rev 59:1-61.

DiGiovanni J. 1992. Multiple carcinogenesis in mouse skin. Pharmacol Ther 54:63-128.

Forte A, Finicelli M, De Luca P, Quarto C, Onorati F, Santè P, Renzulli A, Galderisi U, Berrino L, De Feo M, Rossi F, Cotrufo M, Cascino A, Cipollaro M. 2008. Expression profiles in surgically-induced carotid stenosis: a combined transcriptomic and proteomic investigation. J Cell Mol Med. 12:1956-1973.

Forte A, Grossi M, Turczynska KM, Svedberg K, Rinaldi B, Donniacuo M, Holm A, Baldetorp B, Vicchio M, De Feo M, Santè P, Galderisi U, Berrino L, Rossi F, Hellstrand P, Nilsson BO, Cipollaro M. 2013. Local inhibition of ornithine decarboxylase reduces vascular stenosis in a murine model of carotid injury. Int J Cardiol 168:3370-3380.

Grossi M, Persson L, Swärd K, Turczyńska KM, Forte A, Hellstrand P, Nilsson BO. 2014a. Inhibition of polyamine formation antagonizes vascular smooth muscle cell proliferation and preserves the contractile phenotype. Basic Clin Pharmacol Toxicol 115:379-388.

Grossi M, Rippe C, Sathanoori R, Swärd K, Forte A, Erlinge D, Persson L, Hellstrand P, Nilsson BO. 2014b. Vascular smooth muscle cell proliferation depends on caveolin-1-regulated polyamine uptake. Biosci Rep 34:e00153.

Igarashi K, Kashiwagi K. 2010. Characteristics of cellular polyamine transport in prokaryotes and eukaryotes. Plant Physiol Biochem 48:506-512.

Levin VA, Uhm JH, Jaeckle KA, Choucair A, Flynn PJ, Yung WKA, Prados MD, Bruner JM, Chang SM, Kyritsis AP, Gleason MJ, Hess KR. 2000. Phase III randomized study of postradiotherapy chemotherapy with alpha-difluoromethylornithine-procarbazine, N-(2-chloroethyl)-N'-cyclohexyl-N-nitrosurea, vincristine (DFMO-PCV) versus PCV for glioblastoma multiforme. Clin Cancer Res 6:3878–3884.

Levin VA, Hess KR, Choucair A, Flynn PJ, Jaeckle KA, Kyritsis AP, Yung WK, Prados MD, Bruner JM, Ictech S, Gleason MJ, Kim HW. 2003. Phase III randomized study of postradiotherapy chemotherapy with combination alpha-difluoromethylornithine-PCV versus PCV for anaplastic gliomas. Clin Cancer Res 9:981–990.

Linsalata M, Caruso MG, Leo S, Guerra V, D'Attoma B, Di Leo A. 2002. Prognostic value of tissue polyamine levels in human colorectal carcinoma. Anticancer Res 22:2465-2469.

Lowry OH, Rosebrough NJ, Farr AL, Randall RJ. 1951. Protein measurement with the Folin phenol reagent. J Biol Chem 193: 265–275.

Meyskens FL Jr, McLaren CE, Pelot D, Fujikawa-Brooks S, Carpenter PM, Hawk E, Kelloff G, Lawson MJ, Kidao J, McCracken J, Albers CG, Ahnen DJ, Turgeon DK, Goldschmid S, Lance P, Hagedorn CH, Gillen DL, Gerner EW. 2008. Difluoromethylornithine plus sulindac for the prevention of sporadic colorectal adenomas: a randomized placebo-controlled, double-blind trial. Cancer Prev Res 1:32–38.

Meyskens FL Jr, Gerner EW. 1999. Development of difluoromethylornithine (DFMO) as a chemoprevention agent. Clin Cancer Res 5:945–951.

Miller-Fleming L, Olin-Sandoval V, Campbell K, Ralser M. 2015. Remaining mysteries of Molecular Biology: The role of polyamine metabolites in the cell. J Mol Biol 427:3389-3406.

Mitchell JL, Simkus CL, Thane TK, Tokarz P, Bonar MM, Frydman B, Valasinas AL, Reddy VK, Marton LJ. 2004. Antizyme induction mediates feedback limitation of the incorporation of specific polyamine analogues in tissue culture. Biochem J 384:271-279.

Muth A, Madan M, Archer JJ, Ocampo N, Rodriguez L, Phanstiel O. 2014. Polyamine transport inhibitors: design, synthesis, and combination therapies with difluoromethylornithine. J Med Chem 57:348-363.

Nowotarski SL1, Woster PM, Casero RA Jr: 2013. Polyamines and cancer. implications for chemotherapy and chemoprevention. Expert Rev Mol Med 15:e3.

O'Brien TG. 1976. The induction of ornithine decarboxylase as an early, possibly obligatory event in mouse skin carcinogenesis. Cancer Res 36:2644-2653.

Odenlund M, Holmqvist B, Baldetorp B, Hellstrand P, Nilsson BO. 2009. Polyamine synthesis inhibition induces S phase cell cycle arrest in vascular smooth muscle cells. Amino Acids 36:273-282.

Owens GK. 1995. Regulation of differentiation of vascular smooth muscle cells. Physiol Rev 75:487-517.

Owens GK, Kumar MS, Wamhoff BR. 2004. Molecular regulation of vascular smooth muscle cell differentiation in development and disease. Physiol Rev 84:767-801.

Palacín M, Estévez R, Bertran J, Zorzano A. 1998. Molecular biology of mammalian plasma membrane amino acid transporters. Physiol Rev 78:969-1054.

Pegg AE. 1988. Polyamine metabolism and its importance in neoplastic growth as a target for chemotherapy. Cancer Res 48:759-774.

Pegg AE. 2013. Toxicity of polyamines and their metabolic products. Chem Res Toxicol 26:1782-1800.

Pfaffl MW. 2001. A new mathematical model for relative quantification in real-time RT-PCR. Nucleic Acids Res 29:e45.

Poulin R, Casero RA, Soulet D. 2012. Recent advances in the molecular biology of metazoan polyamine transport. Amino Acids 42:711–723.

Roy UK, Rial NS, Kachel KL, Gerner EW. 2008. Activated K-RAS increases polyamine uptake in human colon cancer cells through modulation of caveolar endocytosis. Mol Carcinog 47:538-553.

Sarhan S, Knodgen B, Seiler N. 1989. The gastrointestinal tract as polyamine source for tumor growth. Anticancer Res 9:215–224.

Seiler N, Daune G, Bolkenius FN, Knödgen B. 1989. Ornithine aminotransferase activity, tissue ornithine concentrations and polyamine metabolism. Int J Biochem 21:425-432.

Sharpe JG, Seidel ER. 2005. Polyamines are absorbed through a y+ amino acid carrier in rat intestinal epithelial cells. Amino Acids 29:245-253.

Soulet D, Covassin L, Kaouass M, Charest-Gaudreault R, Audette M, Poulin R. 2002. Role of endocytosis in the internalization of spermidine-C(2)-BODIPY, a highly fluorescent probe of polyamine transport. Biochem J 367:347-357.

Soulet D, Gagnon B, Rivest S, Audette M, Poulin R. 2004. A fluorescent probe of polyamine transport accumulates into intracellular acidic vesicles via a two-step mechanism. J Biol Chem 279:49355-49366.

Uemura, T, Stringer, DE, Blohm-Mangone KA, Gerner EW. 2010. Polyamine transport is mediated by both endocytic and solute carrier transport mechanisms in the gastrointestinal tract. Am J Physiol Gastrointest Liver Physiol 299:517-522.

Wang Z, Wang DZ, Hockemeyer D, McAnally J, Nordheim A, Olson EN. 2004. Myocardin and ternary complex factors compete for SRF to control smooth muscle gene expression. Nature 428:185-189.

Weiss TS, Bernhardt G, Buschauer A, Thasler WE, Dolgner D, Zirngibl H, Jauch KW. 2002. Polyamine levels of human colorectal adenocarcinomas are correlated with tumor stage and grade. Int J Colorectal Dis 17:381-387.

Welch JE, Bengtson P, Svensson K, Wittrup A, Jenniskens GJ, Ten Dam GB, Van Kuppevelt TH, Belting M. 2008. Single chain fragment anti-heparan sulfate antibody targets the polyamine transport system and attenuates polyamine-dependent cell proliferation. Int J Oncol 32:749-756.

Wessely R. 2010. New drug-eluting stent concepts. Nat Rev Cardiol 7:194-203

Wolak T. 2014. Osteopontin - a multi-modal marker and mediator in atherosclerotic vascular disease. Atherosclerosis 236:327-337.

Wood PL, Khan MA, Moskal JR. 2007. The concept of "aldehyde load" in neurodegenerative mechanisms: cytotoxicity of the polyamine degradation products hydrogen peroxide, acrolein, 3-aminopropanal, 3-acetamidopropanal and 4-aminobutanal in a retinal ganglion cell line. Brain Res 1145:150-156.

Yang Z, Venardos K, Jones E, Morris BJ, Chin-Dusting J, Kaye DM. 2007. Identification of a novel polymorphism in the 3'UTR of the L-arginine transporter gene SLC7A1: contribution to hypertension and endothelial dysfunction. Circulation 115:1269-1274.

Zeidan A, Nordström I, Albinsson S, Malmqvist U, Swärd K, Hellstrand P. 2003. Stretch-induced contractile differentiation of vascular smooth muscle: sensitivity to actin polymerization inhibitors. Am J Physiol Cell Physiol 284:1387-1396.

Figure legends

Fig.1. *Chemical structures of polyamines and polyamine transporter inhibitor (PTI).*
Putrescine (A), spermidine (B), spermine (C) and trimer44NMe/PTI-1 (D).

Fig. 2. *PTI-1 inhibits both basal and DFMO-induced polyamine uptake in mouse VSMCs.*
The cells were pulse-labelled with either [^{3}H]Putrescine (Put, 10 μM) (A) or [^{3}H]Spermidine (Spd, 5 μM) (B) for 30 min after treatment with (open symbol) or without (closed symbol) 5 mM DFMO for 2 days. PTI-1 (0.025-2.5 μM) was introduced together with the radio-labelled polyamines. Two replicate cultures were performed. Data were normalized to uptake of Put (A) or Spd (B) in untreated control cells and given as %. Values are presented as the means ± SEM. n= 6 for each group.

Fig. 3. *PTI-1 inhibits both basal and DFMO-induced polyamine uptake in Cav-1 KO mouse VSMCs.*
The cells were pulse-labelled with either [^{3}H]Put (10 μM) (A) or [^{3}H]Spd (5 μM) (B) for 30 min after treatment with or without 5 mM DFMO for 2 days. PTI-1 (0.5 μM) was introduced together with the radio-labelled polyamines. Two replicate cultures were performed. Values are presented as the means ± SEM. n= 6 for each group. ** and *** represent $P<0.01$ and $P<0.001$, respectively.

Fig. 4. *Treatment with PTI-1 (0.5 μM) and DFMO (5 mM) in combination for 2 days inhibits mouse VSMCs proliferation and completely abolishes cellular Put and Spd contents.*
Cell proliferation was assessed by evaluating cell viability by the CCK-8 assay (A) and cell density by crystal violet staining (B). Cellular polyamine contents were assessed by HPLC (C and D). Two replicate cultures were performed. Values are presented as means ± SEM. n= 6-13 for each group. ** and *** represent $P<0.01$ and $P<0.001$, respectively.

Fig. 5. *Treatment with DFMO (5 mM) alone for a longer time period (4 days) completely abolishes intracellular polyamines and reduces proliferation.*
Cell proliferation was assessed by evaluating cell viability by the CCK-8 assay (A) and cell density by crystal violet (B). PTI-1 was included at 0.5 μM. Cellular polyamine contents were assessed by HPLC (C and D). Two replicate cultures were performed. Values are presented as means ± SEM. n= 6-13 for each group. * and *** represent $P<0.05$ and $P<0.001$, respectively.

Fig. 6. *Analysis of VSMC gene expression after 2 days of treatment with DFMO and PTI-1 alone or in combination.*
Quantitative real-time PCR analysis of gene expression in cells harvested after 2 days of treatment with DFMO (5 mM) and PTI-1 (0.5 μM) alone or in combination. The VSMC contractile marker genes *Cnn1*, *Tagln1* and *Spp1* code for calponin, SM22α and osteopontin, respectively. Two replicate cultures were performed. Data are presented as mean ± SEM. n= 4 for each group. *, ** and *** represent $P < 0.05$, $P<0.01$ and $P<0.001$, respectively.

Fig. 7. *PTI-1 inhibits polyamine uptake and the combination of DFMO+PTI-1 reduces human VSMC proliferation.*
Human VSMCs were pulse-labelled with either [^{3}H]Put (10 μM) (A) or [^{3}H]Spd (5 μM) (B) for 30 min after treatment with or without 5 mM DFMO for 2 days. PTI-1 was introduced together with the radio-labelled polyamines. Cell proliferation was assessed by evaluating cell viability by the CCK-8 assay (C) and cell density by crystal violet (D) after 2 days of treatment with PTI-1 or DFMO alone or in combination. Two replicate cultures were performed. Values are presented as the means ± SEM. n= 6-8 for each group. ** and *** represent $P<0.01$ and $P<0.001$, respectively.

Fig. 8. *Expression of smooth muscle and endothelium differentiation markers is not affected by treatment with DFMO and PTI-1 alone or in combination.*
Mouse aortic rings were cultured for 3 days in DMEM supplemented with 10 nM insulin and 2% dialyzed FBS and treated with DFMO (5 mM) and PTI-1 (1 μM) alone or in combination. Similar immunostaining was observed for the endothelial cell marker vWF (von Willebrand factor) and contractile marker proteins calponin and SM22α in control rings and in rings treated with or without DFMO and PTI-1. The nuclei were stained with DAPI. The scale bar in the upper left panel applies to all images.

Fig. 9. *Treatment with DFMO and the combination of DFMO and PTI-1 inhibits proliferation in cultured mouse aorta.*
Mouse aortic rings were cultured for 3 days in DMEM supplemented with 10 nM insulin and 2% dialyzed FBS and treated with DFMO (5 mM) and PTI-1 (1 μM) alone or in combination. EdU (25μM) was added to the rings 24 h before harvest (green, A). The proportion (%) of EdU-positive cells (i.e., proliferating cells) within the media was determined by counting the EdU-positive cells and normalizing them by the total number of cells (blue, DAPI). Summarized data are presented in panels B and C. The scale bar in the upper left panel in Figure A applies to all images. The EdU-positive cells and total number of VSMC nuclei were determined in 3 sections per mouse. n= 10 mice for each group. * represents $P<0.05$.

Fig. 1

A

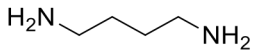

B

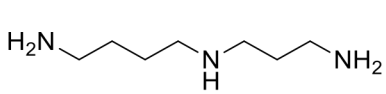

C

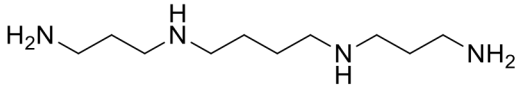

D

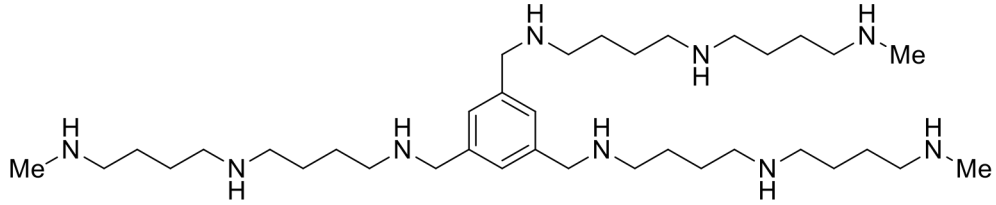

Fig. 2

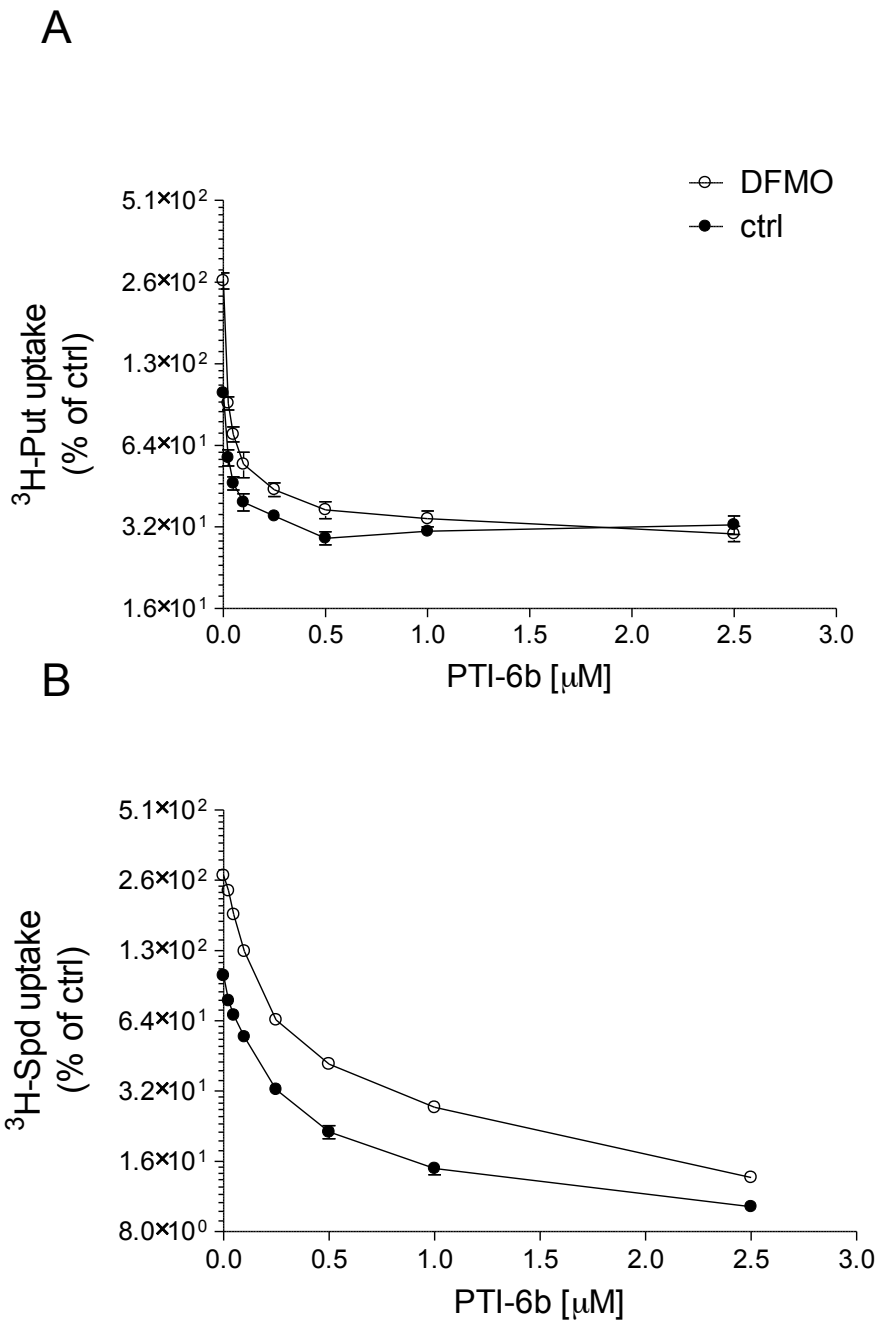
A
DFMO
ctrl
5.1×10²
2.6×10²
1.3×10²
6.4×10¹
3.2×10¹
1.6×10¹
³H-Put uptake
(% of ctrl)
0.0
0.5
1.0
1.5
2.0
2.5
3.0
PTI-6b [μM]
B
5.1×10²
2.6×10²
1.3×10²
6.4×10¹
3.2×10¹
1.6×10¹
8.0×10⁰
³H-Spd uptake
(% of ctrl)
0.0
0.5
1.0
1.5
2.0
2.5
3.0
PTI-6b [μM]

Fig. 3

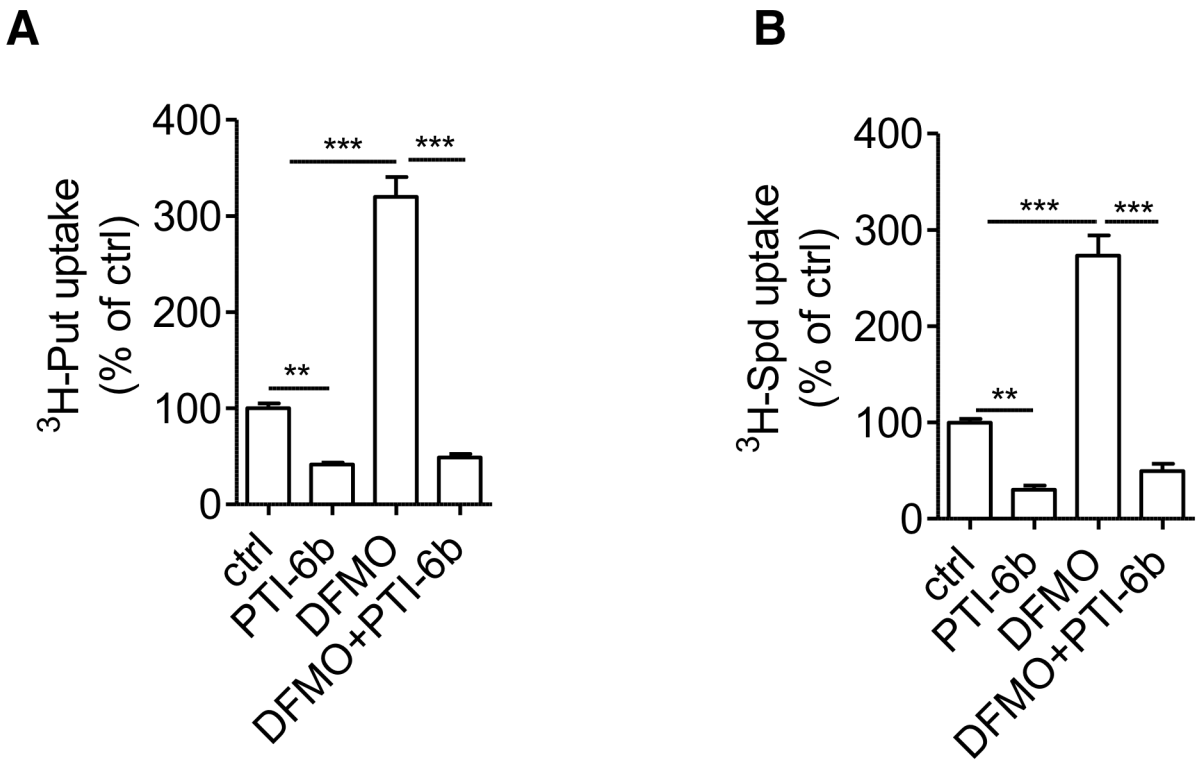
A
B
^{3}H-Put uptake
(% of ctrl)
^{3}H-Spd uptake
(% of ctrl)
400
300
200
100
0
**
***
***
ctrl
PTI-6b
DFMO
DFMO+PTI-6b

Fig. 4

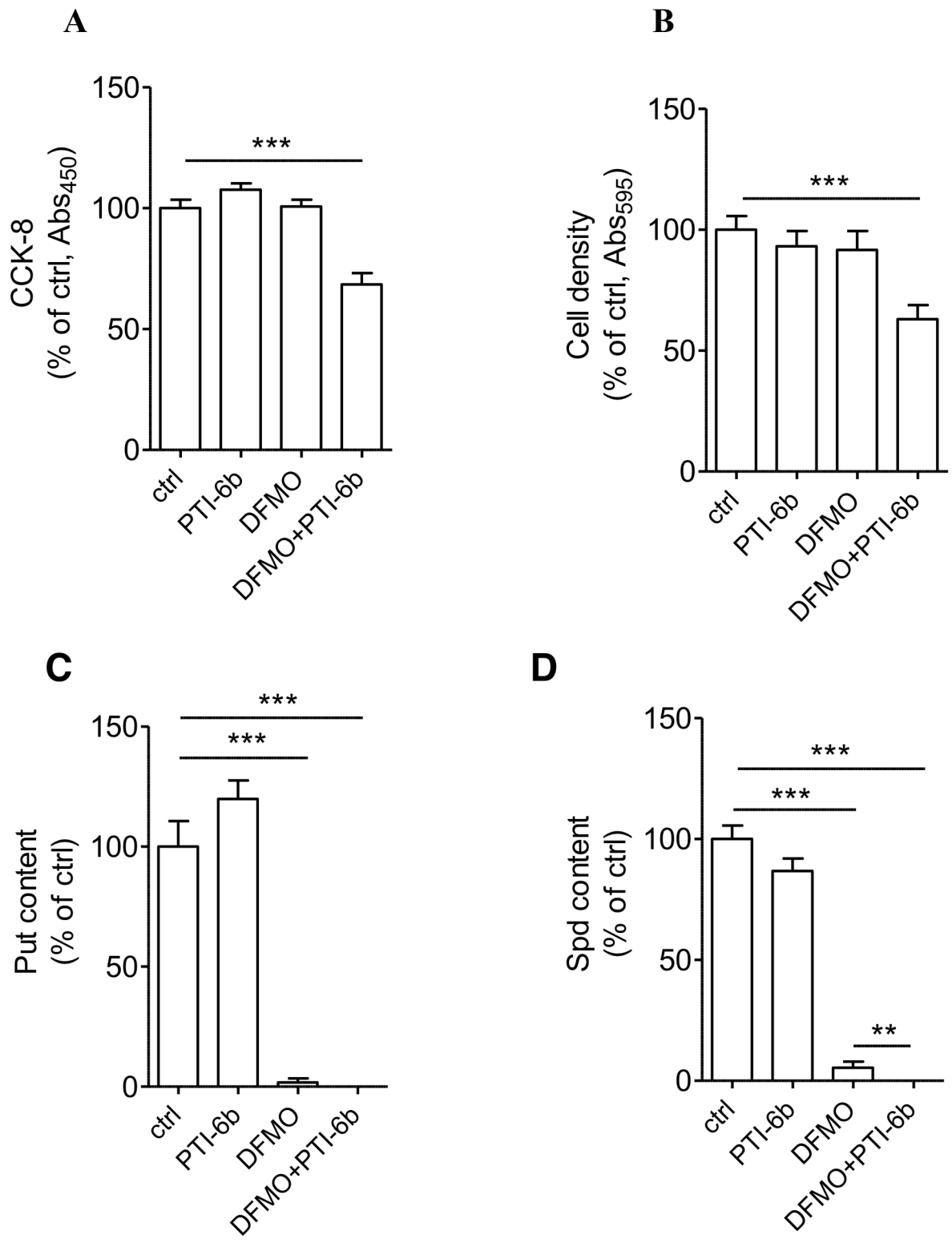
A
CCK-8
(% of ctrl, Abs450)
150
100
50
0
***
ctrl
PTI-6b
DFMO
DFMO+PTI-6b
B
Cell density
(% of ctrl, Abs595)
150
100
50
0
***
ctrl
PTI-6b
DFMO
DFMO+PTI-6b
C
Put content
(% of ctrl)
150
100
50
0
***
***
ctrl
PTI-6b
DFMO
DFMO+PTI-6b
D
Spd content
(% of ctrl)
150
100
50
0
***
***
**
ctrl
PTI-6b
DFMO
DFMO+PTI-6b

Fig. 5

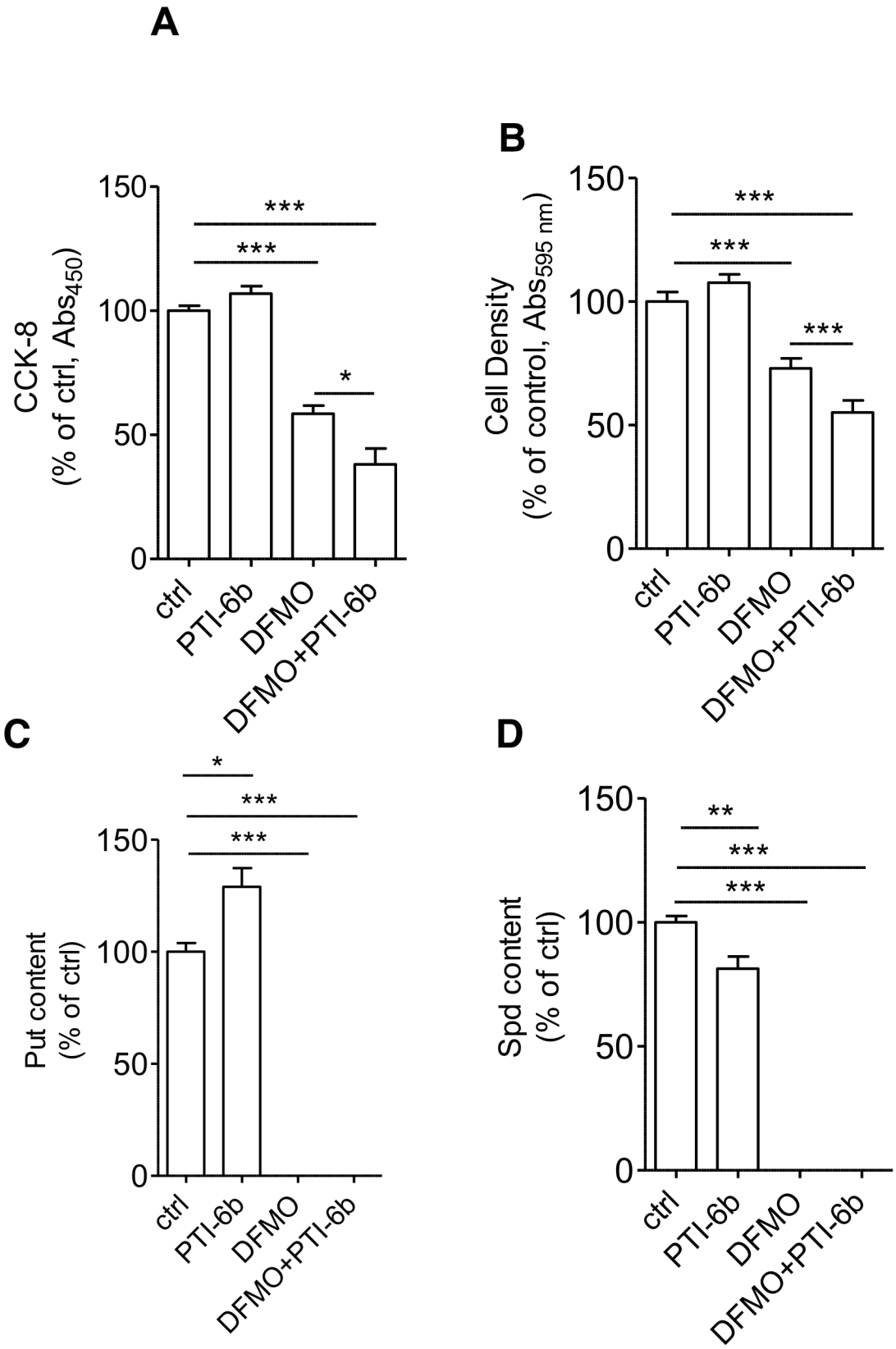
A
CCK-8
(% of ctrl, Abs450)
150
100
50
0
***
***
*
ctrl
PTI-6b
DFMO
DFMO+PTI-6b
B
Cell Density
(% of control, Abs595 nm)
150
100
50
0
***
***
***
ctrl
PTI-6b
DFMO
DFMO+PTI-6b
C
Put content
(% of ctrl)
150
100
50
0
*
***
***
ctrl
PTI-6b
DFMO
DFMO+PTI-6b
D
Spd content
(% of ctrl)
150
100
50
0
**
***
***
ctrl
PTI-6b
DFMO
DFMO+PTI-6b

Fig. 6

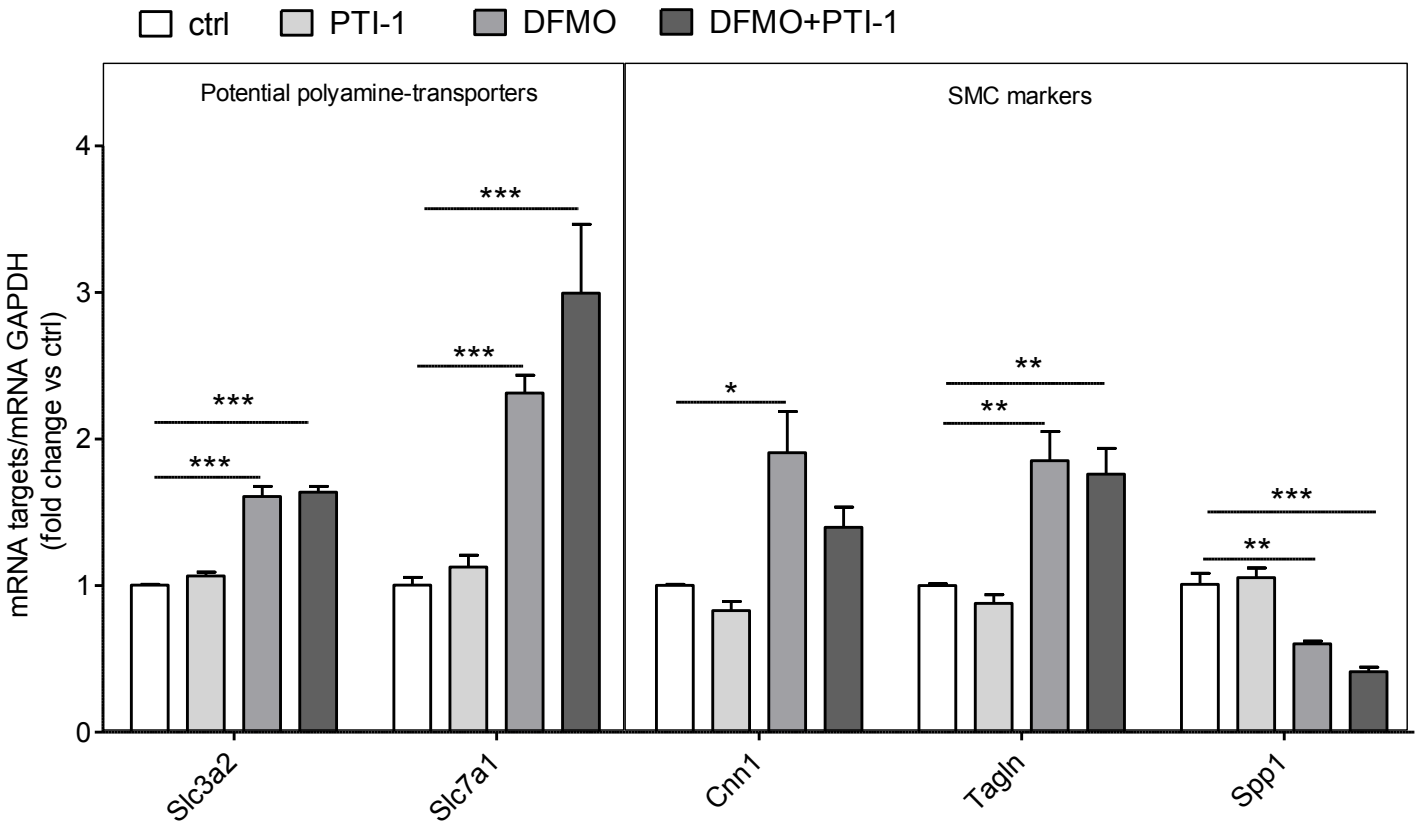
ctrl
PTI-1
DFMO
DFMO+PTI-1
Potential polyamine-transporters
SMC markers
mRNA targets/mRNA GAPDH
(fold change vs ctrl)
0
1
2
3
4
***
***
***
***
*
**
**
***
**
Slc3a2
Slc7a1
Cnn1
Tagln
Spp1

Fig. 7

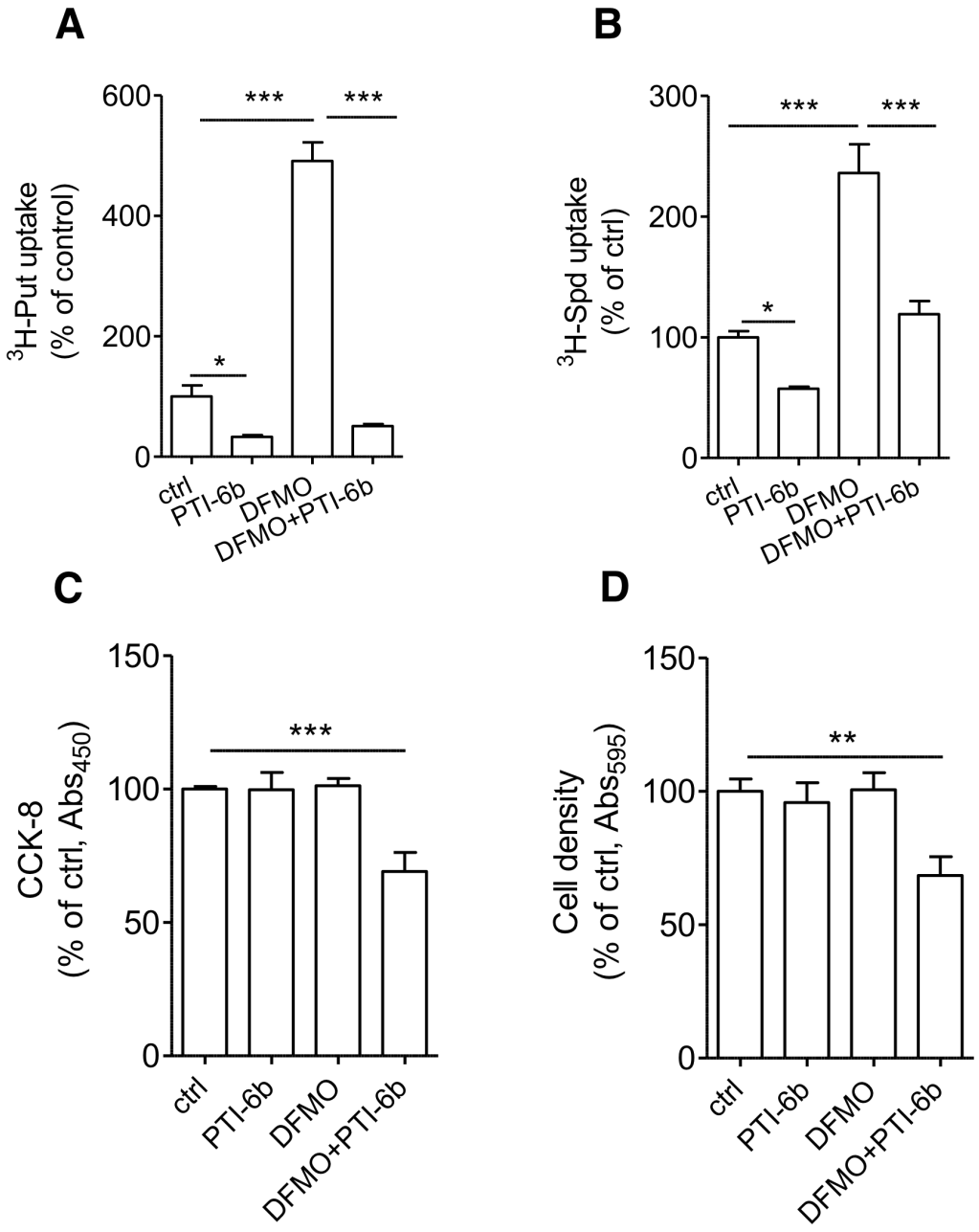
A
B
C
D
^{3}H-Put uptake
(% of control)
^{3}H-Spd uptake
(% of ctrl)
CCK-8
(% of ctrl, Abs$_{450}$)
Cell density
(% of ctrl, Abs$_{595}$)
ctrl
PTI-6b
DFMO
DFMO+PTI-6b
*
**
***

Fig. 8

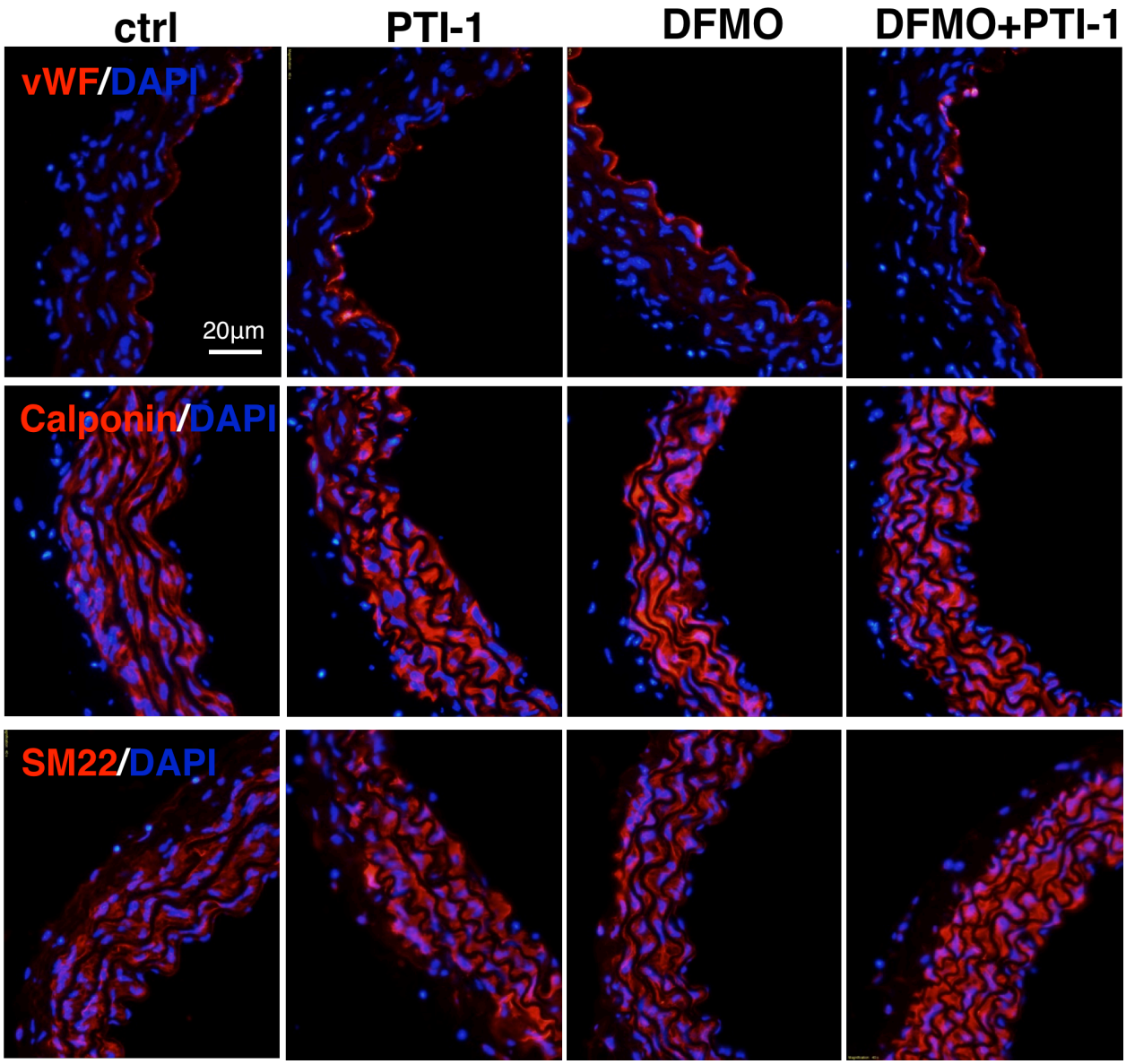
ctrl
PTI-1
DFMO
DFMO+PTI-1
vWF/DAPI
20μm
Calponin/DAPI
SM22/DAPI

Fig. 9

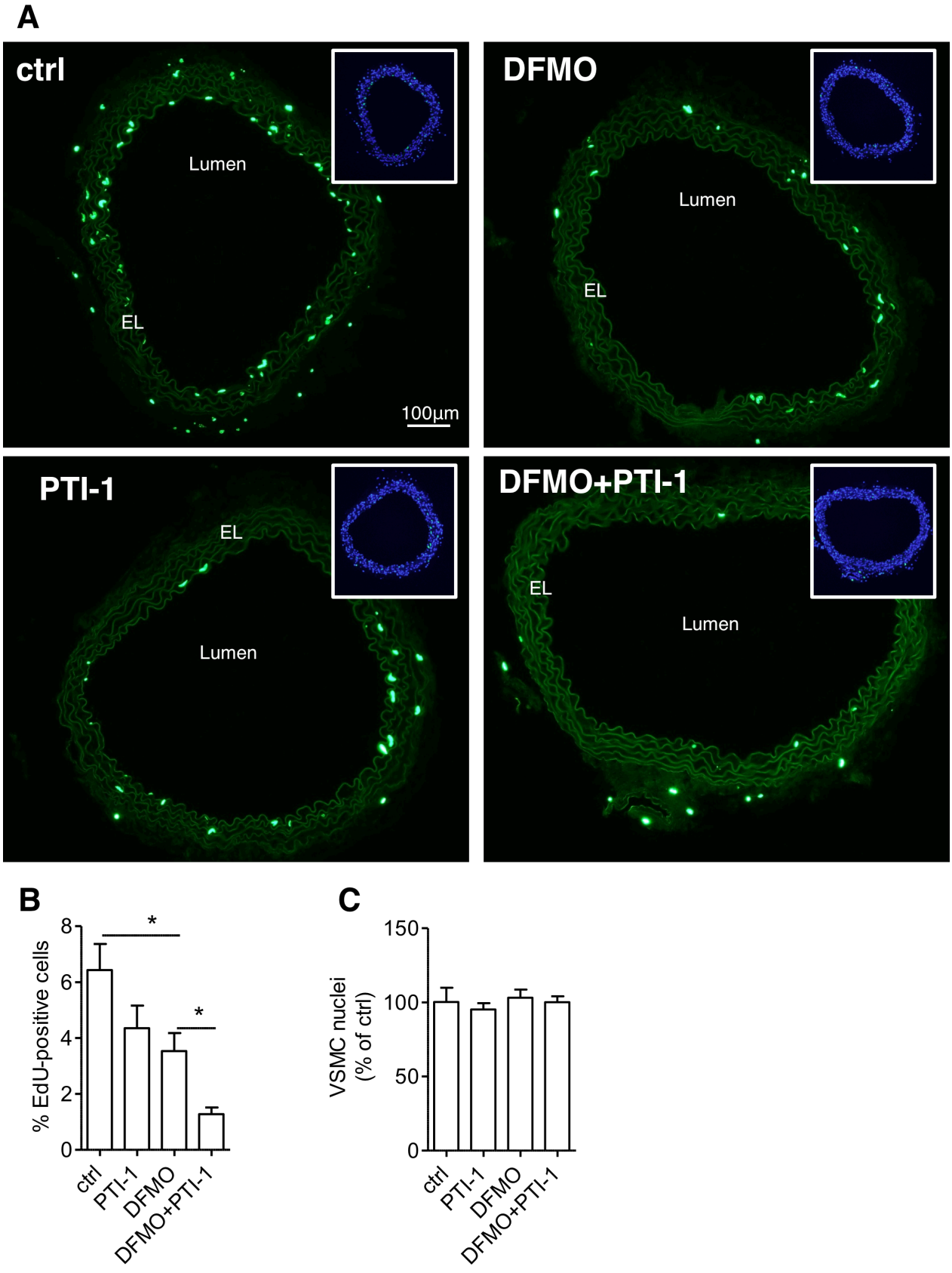
A
ctrl
Lumen
EL
100µm
DFMO
Lumen
EL
PTI-1
EL
Lumen
DFMO+PTI-1
EL
Lumen
B
% EdU-positive cells
0
2
4
6
8
*
*
ctrl
PTI-1
DFMO
DFMO+PTI-1
C
VSMC nuclei (% of ctrl)
0
50
100
150
ctrl
PTI-1
DFMO
DFMO+PTI-1